Molecular Dynamics Studies of the Size, Shape, and Internal Structure of 0% and 90% Acetylated Fifth-Generation Polyamidoamine Dendrimers in Water and Methanol

Hwankyu Lee,[†] James R. Baker, Jr.,[‡] and Ronald G. Larson*[,§]

Department of Biomedical Engineering, Department of Internal Medicine and Nanotechnology Institute for Medicine and the Biological Sciences, and Department of Chemical Engineering, Biomedical Engineering, Mechanical Engineering, and Macromolecular Science and Engineering Program, University of Michigan, Ann Arbor, Michigan 48109

Received: October 26, 2005; In Final Form: December 12, 2005

We have performed molecular dynamics simulations of 0% and 90% acetylated fifth-generation (G5) polyamidoamine (PAMAM) dendrimers in water and methanol and obtained radii of gyration of 2.51−2.57 and 2.11−2.33 nm, respectively, similar to those measured experimentally in methanol by Prosa et al. (*J. Polym. Sci.* **1997**, *35*, 2913−2924) and in water by Choi et al. (*Nano Lett.* **2004**, *4*, 391−397). Calculation of the moments of inertia and the relative shape anisotropy show that both 0% and 90% acetylated G5 are modestly ellipsoidal. The distribution of branch points relative to the center of the dendrimer and penetration of solvent show that the core and surface of the dendrimer are more exposed to water than is the region between the core and the surface due to the interactions between monomers, including hydrogen bonds that rapidly break and re-form as solvent molecules compete for hydrogen-bonding sites on the monomers. The water and methanol solvents seem to produce similar numbers of hydrogen bond interactions between monomers.

Introduction

Polyamidoamine (PAMAM) dendrimers, which contain a central core, regularly branched monomeric building blocks, and many surface terminal groups, are among the best candidate nanoparticles for use as antitumor therapeutics to detect and target tumor cells due to their controlled mass, surface valency, and surface functionality.[1,2] Therefore, such dendrimers are under development as delivery systems for gene or drug delivery,[3,4] and it is important to understand their structure and dynamics in detail. To this end, radii of gyration (R_g) of PAMAM dendrimers of generations G5−G10 have been estimated from electron densities derived from small-angle X-ray scattering (SAXS).[5] The sizes and shapes of these PAMAM dendrimers have also been characterized by transmission electron microscopy (TEM) using biological staining techniques.[6] The effect of solvent quality has been analyzed by measuring R_g using small-angle neutron scattering (SANS) at different solvent ratios of methyl alcohol to acetone and at different temperatures.[7]

While SAXS, SANS, TEM, and other experimental probes provide vital information on the structure of PAMAM dendrimers, results from these are not always easy to interpret at the atomic level. In particular, G5 or lower generations of dendrimers have not been characterized well because of the limited resolution of those experimental techniques. On the other hand, molecular-level phenomena can be visualized in detail by molecular dynamics simulations, which offer insights into structure and dynamics, assuming that these simulations can be validated by successful comparisons to available experimental results.

Molecular dynamics simulations have been performed in a vacuum by Lee et al.[8] on generations G2−G6 PAMAM dendrimers with the different extents of amine protonation that are expected at various pH values. These simulations suggest that the extent of protonation plays an important role in the structure of PAMAM dendrimers. The simulations of Mecke et al.[9] show that PAMAM dendrimers flatten when they come into contact with a negatively charged surface. Maiti et al.[10] simulated generations G1−G11 PAMAM dendrimers and found that the predicted R_g for generation G9 or higher matches those from the experiments. Although these simulations have provided important information, none of them have yielded a value of R_g for a G5 dendrimer that agrees with the experimental result, presumably because, to save computer time, the simulations were carried out either in a vacuum or in a dielectric medium rather than in explicit water. The Goddard group has performed molecular dynamics simulations of dendrimers in water solvent. For example, Maiti et al.[11] carried out simulations in water of G4−G6 PAMAM dendrimers. While these simulations provide valuable insights, the simulation time was only 400 ps, which does not yield an equilibrated system or adequate sampling. Similarly, Lin et al.[12] showed that the thermodynamic and dynamic properties of water near G5 PAMAM dendrimers are different from those of bulk water. However, the simulations did not determine the conformation and interactions of the equilibrated dendrimer in water, presumably because of insufficient run times. Recently, Han et al.[13] simulated G1−G7 PAMAM dendrimers in explicit water for 4.5−15 ns and showed that there are significant structural differences between results using implicit vs explicit solvent. However, they did not compare the R_g values from their simulated dendrimers with

* Corresponding author. E-mail: rlarson@umich.edu.
[†] Department of Biomedical Engineering.
[‡] Department of Internal Medicine and Nanotechnology Institute for Medicine and the Biological Sciences.
[§] Department of Chemical Engineering, Biomedical Engineering, Mechanical Engineering, and Macromolecular Science and Engineering Program.

10.1021/jp056148s CCC: $33.50
Published on Web 02/03/2006

TABLE 1: List of Simulations[a]

dendrimer type	generation	number of surface groups		total charge	number of atoms in dendrimer	solvent	simulation time (ns)
		NH_3^+	acetylation ($NHCOCH_3$)				
G5	5	128		128	4676	water	4.9
G5M	5	128		128	4676	methanol	4.5
G5-Ac90	5	12	116	12	5140	water	6.4
G5M-Ac90	5	12	116	12	5140	methanol	5.0

[a] G5 and G5M indicate 0% acetylated G5 PAMAM dendrimers (EDA core) with protonated surface residues, in water and methanol, respectively. "G5-Ac90" and "G5M-Ac90" are 90% acetylated G5 PAMAM dendrimers, in water and methanol, respectively.

the experimental values, because in their simulations the amines were unprotonated, rather than being protonated as is the case at the physiological and experimental pH of 7. More importantly, their simulations were performed in water rather than in methanol, which was used in the experiments of Prosa et al.[5] Therefore, to date, simulations have not yielded R_g values that can realistically be compared to the experimental values. In addition, interactions between branches of a dendrimer in different solvents have not yet been analyzed and understood at the atomic level, especially for the G5 PAMAM dendrimer, which has been widely studied for gene or drug delivery applications. While the surface amines of unmodified G5 PAMAM dendrimers are protonated at pH 7, these amines are often 80−90% acetylated to prevent nonspecific interactions of the dendrimers with cells.[14,15] Therefore, acetylated G5 dendrimers have been widely used for nanoparticle targeting of anticancer drug and self-assembly of dendrimers using complementary single-stranded oligonucleotides.[4,16,17] Here, we perform 4.5−6.4-ns-long molecular dynamics simulations of the structure of 0% and 90% acetylated G5 PAMAM dendrimers with protonated surface amines in explicit water and methanol to investigate atomic-scale interactions of the dendrimer with solvent as well as dendrimer shape and size, which we compare with experimental findings.

Methods

Initial atomic coordinates for 0% and 90% acetylated G5 PAMAM dendrimers (EDA core) were generated using the Insight II software package (Accelrys Inc., San Diego, CA), followed by several steps of energy minimization. Characteristics of 0% and 90% acetylated G5 dendrimers are listed in Table 1. All simulations were performed using the AMBER8 simulation package with the general AMBER force field (GAFF)[18,19] and the TIP3PBOX water model,[20] and all analyses were performed by using AMBER8 and GROMACS simulation package tools.[21] Our simulations were carried out in a truncated octahedral box, whose faces consist of eight hexagons and six squares, with water molecules packed around a single dendrimer molecule placed at the center of the box, with at least 8 Å between any atom of the dendrimer and the edge of the box. Periodic boundary conditions were used. We included 27 085 and 19 345 water molecules respectively for the 0% and 90% acetylated dendrimers. As counterions, 128 Cl^- and 12 Cl^- ions respectively were also added to the boxes containing 0% and 90% acetylated dendrimers to make the corresponding systems neutral. A total of 86 059 and 63 187 atoms respectively were therefore used for the 0% and 90% acetylated dendrimers. For the systems with the methanol solvent, the same procedures were performed with different numbers of solvent molecules.

The temperature was maintained at 298 K by applying Langevin dynamics,[22] and an NPT ensemble was used. A cutoff of 9 Å was used for van der Waals interactions and particle mesh Ewald summation (PME) for electrostatic interactions.[23] SHAKE constraints were applied to all bonds involving hydrogen atoms.[24] After energy minimizations with and without restraints on the dendrimer molecules, equilibration runs were performed for 4.5−6.4 ns, with a time step of 2 fs. Radii of gyration and principal moments of inertia of the dendrimers in our simulations do not change after 2.5−4 ns. In addition, the autocorrelation functions of radius of gyration yield a relaxation time below 1.5 ns, which is consistent with that found by Han et al.[13] Also, radii of gyration and principal moments of inertia obtained from the last 500 ps show very small errors, estimated by using block averaging, suggesting that the systems are equilibrated well. The coordinates were saved every picosecond for analysis.

Results and Discussion

We performed molecular dynamics simulations of 0% and 90% acetylated G5 PAMAM dendrimers in explicit water and methanol. Here, these dendrimers are named "G5", "G5M", "G5-Ac90", and "G5M-Ac90", and details describing them are given in Table 1. Figure 1 shows snapshots from the beginning (top image) and end (bottom image) of the simulations. Final conformations show that all the dendrimers shrink and form ellipsoidal spheroids, with G5-Ac90 and G5M-Ac90 becoming more compact than G5 and G5M. To investigate the size and shape, water distribution, and hydrogen bond interactions, the average properties were analyzed over the last 500 ps, when the system is in its most equilibrated state.

Size and Shape of Dendrimers. To analyze the size of the dendrimers quantitatively, the radii of gyration R_g were calculated and compared with values from experiments and from other simulations. R_g has been measured using electron densities obtained from SAXS by Prosa et al.,[5] and thus we modified the normal equation for R_g by using electron numbers instead of mass. (Here, $R_g = (\sum_i ||r_i||^2 e_i / \sum_i e_i)^{1/2}$, where e_i is the electron number and r_i is the position of atom i with respect to the center of mass of the molecule).

Figure 2a shows that R_g values for G5, G5M, G5-Ac90, and G5M-Ac90 drastically decrease as functions of time at the beginning of the simulations and then reach apparent steady-state values of 2.5, 2.6, 2.1, and 2.3 nm at around 2.5, 3.5, 4, and 4 ns, respectively. In Figure 2b, autocorrelation functions, $C_{R_g}(t)$, for R_g yield relaxation times, defined as the time at which $C_{R_g}(t) = 1/e$, and these are below 1.5 ns, suggesting that dendrimers are equilibrated within the simulated time scales. Han et al. also found that R_g for their dendrimers in explicit water stabilized within 1.5 ns.[13] Table 2 shows that the values of R_g from our simulations compare favorably with those from experiments. Prosa et al.[5] used SAXS to measure a value of 2.41 nm for the radius of gyration of dilute G5 in methanol, while Choi et al.[26] used size-exclusion chromatography to measure values of 2.5 and 2.35 nm for G5 and G5-Ac90 in a mixture of water and citric acid. We note that G5 dendrimers are too small for these methods to be expected to give exact

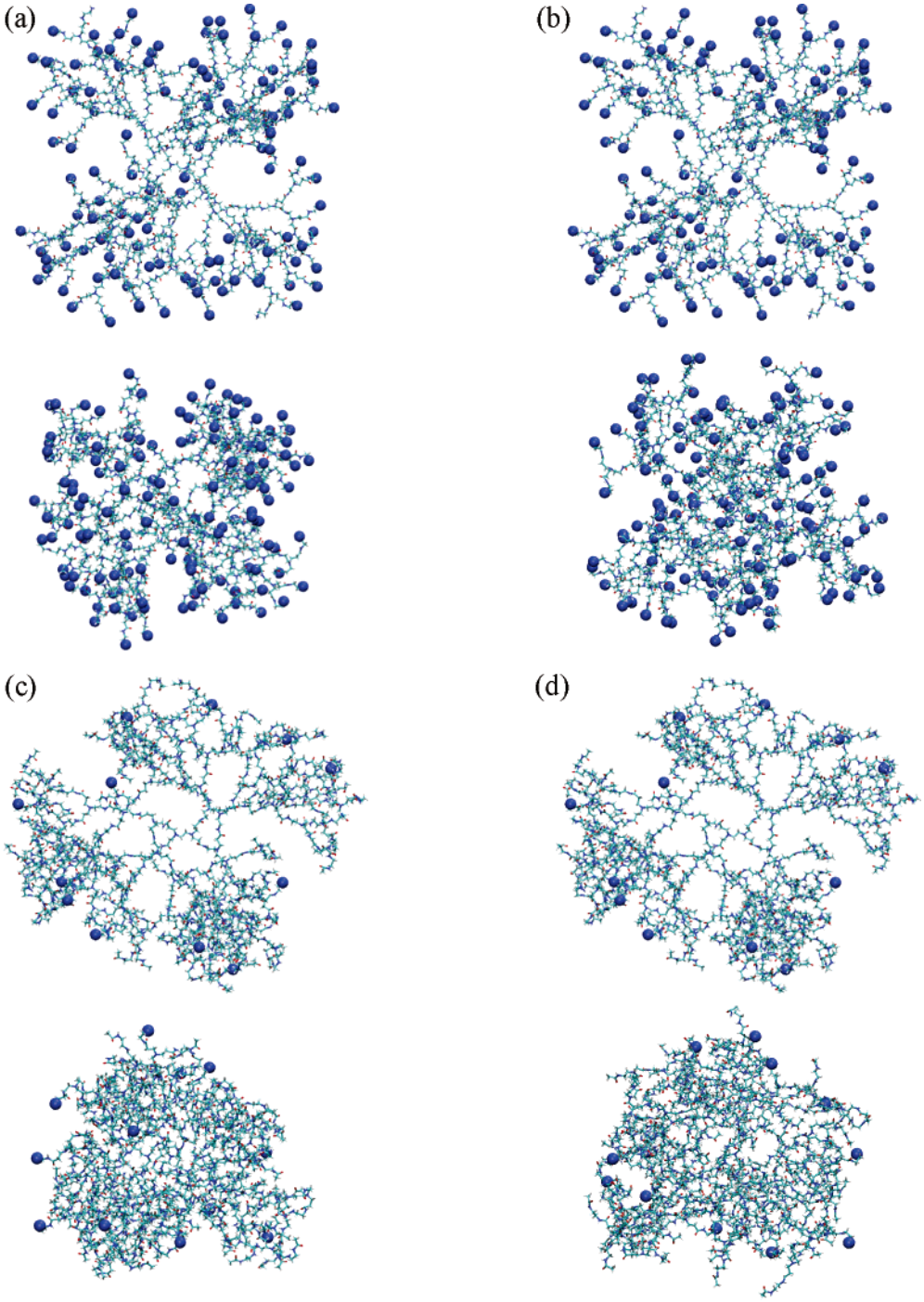

Figure 1. Snapshots at the beginning (0 ns, top images) and end (4.9 ns for G5, 4.5 ns for G5M, 6.4 ns for G5-Ac90, and 5.0 ns for G5M-Ac90, bottom images) of (a) G5, (b) G5M, (c) G5-Ac90, and (d) G5M-Ac90 simulations. Protonated surface residues (NH_3^+) are shown as blue dots. The explicit water molecules and counterions are omitted for clarity. The images ware created using VMD.[25]

TABLE 2: Average Values of Radius of Gyration (R_g) of G5, G5M, G5-Ac90, and G5M-Ac90 over the Last 500 ps of the Simulations, Compared with Experiments and Other Simulations

	radius of gyration (nm)					
	experiment		simulation			
	Prosa et al.[5]	Choi et al.[26]	This work	Maiti et al.[11]	Lee et al.[8,a]	Maiti et al.[10,a]
G5		2.50	2.51 ± 0.01	2.22 ± 0.01	3.28	1.83
G5M	2.41		2.57 ± 0.01			
G5-Ac90		2.35	2.11 ± 0.01			
G5M-Ac90			2.33 ± 0.01			

[a] These simulations were performed without explicit water.

radii of gyration; however, our simulations seem to confirm that these measurements are, in fact, reasonably accurate.

On the other hand, simulations in a vacuum by Lee et al.[8] and Maiti et al.[10] yielded radii of gyration of 3.28 and 1.83 nm,

TABLE 3: Average Values of the Principal Moments of Inertia, Aspect Ratio, and Relative Shape Anisotropy of G5, G5M, G5-Ac90, and G5M-Ac90 over the Last 500 ps of the Simulations

	I_z (a.m.u. nm^2)	I_y (a.m.u. nm^2)	I_x (a.m.u. nm^2)	I_z/I_y	I_z/I_x	relative shape anisotropy
G5	146 071 ± 617	117 285 ± 485	100 815 ± 2 629	1.25	1.45	0.01
G5M	143 862 ± 1 626	120 815 ± 1 703	115 610 ± 436	1.19	1.24	0.01
G5-Ac90	131 178 ± 251	91 931 ± 548	76 454 ± 215	1.43	1.72	0.03
G5M-Ac90	76 752 ± 878	64 286 ± 914	56 690 ± 333	1.19	1.35	0.01

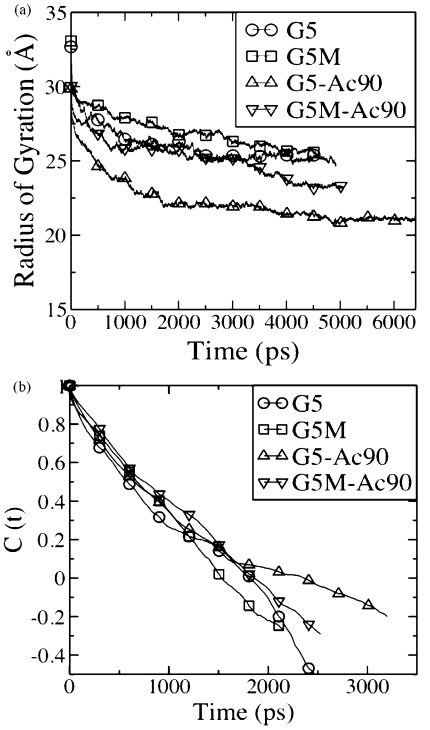

Figure 2. (a) Radii of Gyration (R_g) and (b) autocorrelation function ($C(t)$) of R_g of G5, G5M, G5-Ac90, and G5M-Ac90 as functions of time.

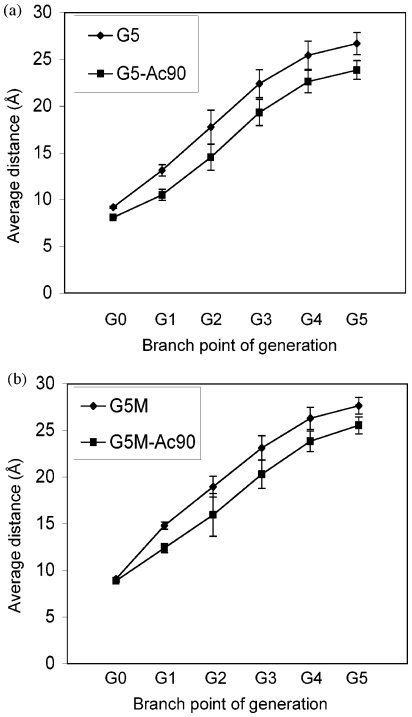

Figure 3. Average distance between N atoms of branch points and center of mass of G0 in (a) water and (b) methanol over the last 500 ps of simulations. G0−G5 represent N atoms positioned in the terminals of generations 0−5 of the dendrimer.

respectively, for these dendrimers, which do not agree with the experimental values. Han et al. simulated a G5 dendrimer in explicit water, but the dendrimer was unprotonated, and the value of R_g they obtained was 1.7 nm, which also disagrees with the experimental result. Maiti et al.[11] determined a radius of gyration of 2.22 nm in explicit water, which is smaller than the value from our simulations and the experimental result. The difference in the value of R_g between our work and theirs might be due to the use of different force fields, their use of mass instead of electron number to calculate R_g, and the short run time used by Maiti et al. Our results both in water and in methanol agree with the experimental values and indicate that acetylation makes dendrimers more compact, apparently by reducing the number of repulsive charged surface groups. Although in methanol dendrimers are slightly less compact than in water, the difference in R_g values between the two solvents is small.

In addition to determining the sizes of the dendrimers, we computed their aspect ratios, I_z/I_x and I_z/I_y, where I_z, I_y, and I_x are principal moments of inertia, ordered such that $I_z > I_y > I_x$, and obtained the relative shape anisotropy, κ^2 ($\kappa^2 = 1 - 3I_2/I_1^2$, where I_1 and I_2 are the first and second invariants of the radius of gyration tensor ($I_1 = I_x + I_y + I_z$, $I_2 = I_xI_y + I_yI_z + I_xI_z$)). A linear array of skeletal atoms is characterized by $\kappa^2 = 1$, while a molecule with tetrahedral or higher symmetry is characterized by $\kappa^2 = 0$.[27] Table 3 shows average values of the principal moments of inertia, aspect ratio, and relative shape anisotropy of dendrimers averaged over the last 500 ps of the simulations. The aspect ratios, I_z/I_y and I_z/I_x, are 1.19−1.43 and 1.24−1.72, respectively, showing that both acetylated and un-acetylated dendrimers have modestly ellipsoidal shapes. The values of the relative shape anisotropies are 0.01−0.03, showing them to be roughly spherical, suggesting that acetylation and change in solvent from water to methanol do not significantly affect the shape of the dendrimers.

Distributions of Branch Points and Solvents. We analyzed the distribution of branch points to understand the conformation of dendrimers. Figure 3 shows the average distance between the nitrogen atoms positioned at the terminals of each generation (G0−G5 indicate N atoms positioned at the terminals of generations 0−5) and the core of the dendrimer, which is defined as the center of mass of all atoms in generation 0. The acetylated and un-acetylated dendrimers have similar distances between the N atoms of G0 and the core of the dendrimer; however, un-acetylated dendrimers have larger distances between G1−G5 N atoms and the core than do acetylated dendrimers, which is consistent with the observation that acetylation reduces R_g. As the generation of the branch point increases, we find that the average distance between the N atoms of the branch points and the core linearly increases from G0 to G4, which is not seen in the work of Maiti et al.[11] Maiti et al. find that in their simulations the branch point of G2 resides much farther from the core than does the branch point of G1 and is even farther from the core than that of G3. This highly nonlinear trend observed by Maiti et al. might result from their small simulation

TABLE 4: Numbers of O Atoms of Solvents Per Branch Point (Water for G5 and G5-Ac, Methanol for G5M and G5M-Ac90) within 5 Å of Branch-Point N Atoms, Averaged over All Branch Points in a Given Generation[a]

	average number of O atoms of solvents					
	G0	G1	G2	G3	G4	G5
G5	4.52 ± 0.12	3.56 ± 0.11	2.75 ± 0.03	2.21 ± 0.05	3.51 ± 0.07	8.95 ± 0.13
G5M	4.17 ± 0.09	2.81 ± 0.05	2.63 ± 0.10	2.53 ± 0.03	2.95 ± 0.03	5.38 ± 0.08
G5-Ac90	2.21 ± 0.13	1.37 ± 0.06	1.04 ± 0.04	1.18 ± 0.03	1.68 ± 0.04	2.94 ± 0.04
G5M-Ac90	2.27 ± 0.07	1.89 ± 0.14	2.00 ± 0.13	1.75 ± 0.02	2.19 ± 0.02	3.30 ± 0.01

[a] G0−G5 represent N atoms positioned at the terminals of the zeroth to fifth generations of the dendrimer.

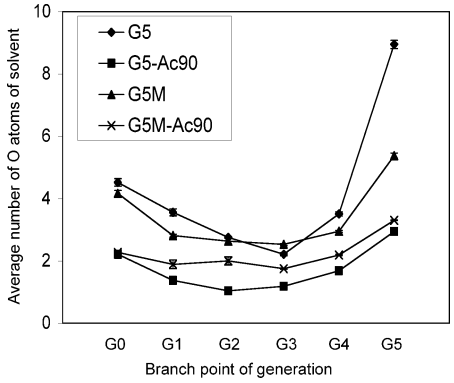

Figure 4. Average number of O atoms of solvents within 5 Å of branch points, N atoms, as a function of branch point location.

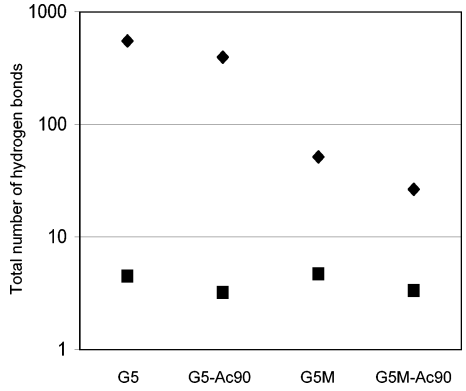

Figure 5. Sum of all hydrogen bonds formed either between monomers of the dendrimer and solvent (♦), or between different monomers of the dendrimer (■), averaged over the last 500 ps of the simulation.

time scale. In Figure 3, note that the positions of the N atoms in G4 and G5 overlap, whereas those in G0−G3 do not, suggesting that the monomers in G5 strongly interact with those in G4, which was also observed in the work of Maiti et al.[11]

In addition to the distribution of branch points, we analyzed the distribution of solvent molecules, either water or methanol, inside the dendrimer. Maiti et al.[11] found that there are four water molecules per tertiary amine in G5 dendrimer at neutral pH; however, the distributions of water molecules near amines for different generation branch points were not computed. Table 4 shows the numbers of O atoms of water and methanol per branch point within 5 Å of the nitrogen atoms at the branch points, averaged over all branch points in a given generation. In Figure 4, G1−G4 have fewer solvent molecules within 5 Å of the branch-point N atoms than do G0 and G5, suggesting that the core and surface of a denrdrimer are more exposed to water than is the region between the core and surface, which is denser in dendrimer mass due to the interactions between dendrimer branches. Especially, G2 and G3 have many fewer nearby solvent molecules per branch point, suggesting greater dendrimer density there.

In addition, branch points in the acetylated dendrimers G5-Ac90 and G5M-Ac90 have many fewer nearby solvent molecules than do G5 and G5M, apparently due to greater compactness of acetylated dendrimers, observed in the lower value of R_g. These results suggest that interactions between branches in a dendrimer and the interactions between branches and solvent may play an important role in the final conformation of the dendrimer. To understand these interactions more thoroughly, we next analyze the formation of hydrogen bonds.

Hydrogen-Bonding Interactions. While the dendrimers consist of uncharged hydrophobic monomers, each monomer has one CO and one NH group, each of which can form hydrogen bonds with other monomers. Our criteria for the existence of a hydrogen bond are that the hydrogen-acceptor distance is less than 0.25 nm and the angle of the donor−hydrogen−acceptor triplet is more than 120°.[28]

There are 636 donors and 758 acceptors in G5 and G5M, and there are 404 donors and 874 acceptors in G5-Ac90 and G5M-Ac90, which can form hydrogen bond interactions. Hydrogen bond existence maps show that each hydrogen-bonding site exchanges partners 30−50 times during the roughly 5-ns simulation, with different water or methanol molecules competing for bonding sites with the dendrimer. We analyzed quantitatively the average lifetime of the hydrogen bonds from the integral over the autocorrelation function of the hydrogen-bonding existence functions (either 0 or 1) averaged over all hydrogen bonds.[21] Average hydrogen bond lifetimes were measured over the last 500 ps of the simulations, showing that lifetimes of hydrogen bonds either between dendrimer monomers and solvent or between dendrimer monomers are almost equally short, in the range of 0.5−0.57 ps, suggesting that the competition between the dendrimer and solvent for the same binding sites leads to the fast formation and breaking of the hydrogen bonds.

Figure 5 shows the total number of hydrogen bonds formed either between a dendrimer monomer and a solvent molecule, or between two dendrimer monomers, averaged over the last 500 ps of the simulations. While each dendrimer forms 395−552 hydrogen bonds with water molecules, each dendrimer forms only 26−52 hydrogen bonds with methanol molecules. Although water molecules have more hydrogen bond interactions with dendrimers than do methanol molecules, a total of only around 3−5 hydrogen bonds form between two different dendrimer monomers when the dendrimer is in either water or methanol, suggesting that the water and methanol produce similar numbers of intra-dendrimer hydrogen bonds. Figure 6 shows a snapshot of the hydrogen bond interaction between CO of G4 and NH groups of G5 in G5-Ac90, showing that the hydrogen bonds between these two groups bring them closer together, making the dendrimer more compact.

Conclusions

We performed molecular dynamics simulations of 0% and 90% acetylated G5 PAMAM dendrimers in explicit water and explicit methanol for 4.5−6.4 ns and found that their radii of

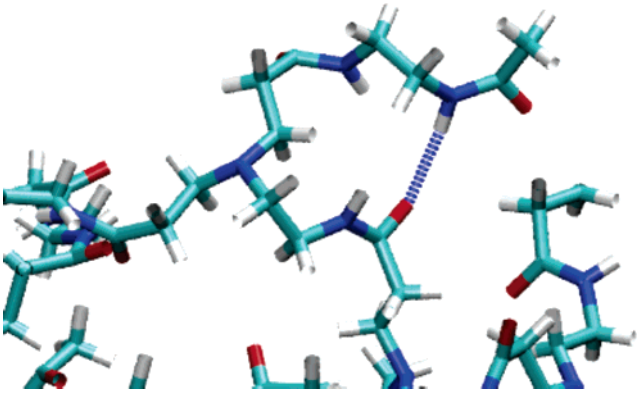

Figure 6. Snapshot of the hydrogen bond interaction between an O atom of G4 and an NH atom of G5 in G5-Ac90. Light blue regions represent C atoms, dark blue represent N atoms, red regions represent O atoms, white regions represent H atoms, and a dotted line represents a hydrogen bond. The water molecules are omitted for clarity.

gyration, R_g, are 2.51−2.57 and 2.11−2.33 nm for 0% and 90% acetylated G5 dendrimers, respectively, which correspond closely to the experimental results for both water and methanol. The radii of gyration and moments of inertia show that both acetylated and un-acetylated dendrimers have modestly ellipsoidal shapes. Distributions of branch points of dendrimers and O atoms of solvents show that the core and surface of the denrdrimer are more exposed to water, whereas the intermediate region is denser without much penetration of solvent. In addition, hydrogen bonds between monomers of the dendrimers, form, break, and re-form, competing with solvent for hydrogen-bonding sites, yielding an average of 3−5 hydrogen bonds between the monomers of a single dendrimer. Differences between water and methanol do not significantly affect the size and shape of the dendrimers and the properties of the hydrogen-bonding interactions between monomers.

Acknowledgment. We gratefully acknowledge the help of Bernell Williams and Youngseon Choi in the laboratory of James Baker with the use of INSIGHTII software. Partial research support was provided by the National Cancer Institute, National Institutes of Health, under contract no. N01-CO-97111.

References and Notes

(1) Baker, J. R.; Quintana, A.; Piehler, L. T.; Holl, M. M. B.; Tomalia, D. A.; Raczka, E. *Biomed. Microdevices* **2001**, *3*, 61−69.

(2) Tomalia, D. A.; Naylor, A. M.; Goddard, W. A. *Angew. Chem., Int. Ed. Engl.* **1990**, *29*, 138−175.

(3) Malik, N.; Evagorou, E. G.; Duncan, R. *Anti-Cancer Drugs* **1999**, *10*, 767−776.

(4) Choi, Y.; Thomas, T.; Kotlyar, A.; Islam, M. T.; Baker, J. R. *Chem. Biol.* **2005**, *12*, 35−43.

(5) Prosa, T. J.; Bauer, B. J.; Amis, E. J.; Tomalia, D. A.; Scherrenberg, R. *J. Polym. Sci.* **1997**, *35*, 2913−2924.

(6) Jackson, C. L.; Chanzy, H. D.; Booy, F. P.; Drake, B. J.; Tomalia, D. A.; Bauer, B. J.; Amis, E. J. *Macromolecules* **1998**, *31*, 6259−6265.

(7) Topp, A.; Bauer, B. J.; Tomalia, D. A.; Amis, E. J. *Macromolecules* **1999**, *32*, 7232−7237.

(8) Lee, I.; Athey, B. D.; Wetzel, A. W.; Meixner, W.; Baker, J. R. *Macromolecules* **2002**, *35*, 4510−4520.

(9) Mecke, A.; Lee, I.; Baker, J. R.; Banaszak Holl, M. M.; Orr, B. G. *Eur. Phys. J. E* **2004**, *14*, 7−16.

(10) Maiti, P. K.; Cagin, T.; Wang, G.; Goddard, W. A. *Macromolecules* **2004**, *37*, 6236−6254.

(11) Maiti, P. K.; Cagin, T.; Lin, S. T.; Goddard, W. A. *Macromolecules* **2005**, *38*, 979−991.

(12) Lin, S.; Maiti, P. K.; Goddard, W. A. *J. Phys. Chem. B* **2005**, *109*, 8663−8672.

(13) Han, M.; Chen, P.; Yang, X. *Polymer* **2005**, *46*, 3481−3488.

(14) Majoros, I. J.; Keszler, B.; Woehler, S.; Bull, T.; Baker, J. R. *Macromolecules* **2003**, *36*, 5526−5529.

(15) Quintana, A.; Raczka, E.; Piehler, L.; Lee, I.; Myc, A.; Majoros, I.; Patri, A. K.; Thomas, T.; Mule, J.; Baker, J. R. *Pharm. Res.* **2002**, *19*, 1310−1316.

(16) Kukowska-Latallo, J. F.; Candido, K. A.; Cao, Z. Y.; Nigavekar, S. S.; Majoros, I. J.; Thomas, T. P.; Balogh, L. P.; Khan, M. K.; Baker, J. R. *Cancer Res.* **2005**, *65*, 5317−5324.

(17) Islam, M. T.; Majoros, I. J.; Baker, J. R. *J. Chromatogr. B* **2005**, *822*, 21−26.

(18) Case, D. A.; Darden, T. A.; Cheatham, T. E.; Simmering, C. L.; Wang, J.; Duke, R. E.; Luo, R.; Merz, K. M.; Wang, B.; Pearlman, D. A.; Crowley, M.; Brozell, S.; Tsui, V.; Gohlke, H.; Mongan, J.; Hornak, V.; Cui, G.; Beroza, P.; Schafmeister, C.; Caldwell, J. W.; Ross, W. S.; Kollman, P. A. *AMBER8*; 2004.

(19) Wang, J.; Wolf, R. M.; Caldwell, J. W.; Kollman, P. A.; Case, D. A. *J. Comput. Chem.* **2004**, *25*, 1157−1174.

(20) Jorgensen, W. L. *J. Am. Chem. Soc.* **1981**, *103*, 335−340.

(21) Lindahl, E.; Hess, B.; van der Spoel, D. *J. Mol. Model.* **2001**, *7*, 306−317.

(22) Pastor, R. W.; Brooks, B. R.; Szabo, A. *Mol. Phys.* **1988**, *65*, 1409−1419.

(23) Essmann, U. L.; Perera, L.; Berkowitz, M. L.; Darden, T.; Lee, H.; Pedersen, L. G. *J. Chem. Phys.* **1995**, *103*, 8577−8592.

(24) Ryckaert, J. P.; Ciccotti, G.; Berendsen, H. J. C. *J. Comput. Phys.* **1977**, *23*, 327−336.

(25) Humphrey, W.; Dalke, A.; Schulten K. *J. Mol. Graphics* **1996**, *14*, 33−38.

(26) Choi, Y.; Mecke, A.; Orr, B. G.; Banaszak Holl, M. M.; Baker, J. R. *Nano Lett.* **2004**, *4*, 391−397.

(27) Theodorou, D. N.; Suter U. W. *Macromolecules* **1985**, *18*, 1206−1214.

(28) Jeffrey, G. A.; Saenger, W. *Hydrogen Bonding in Biological Structures*; Springer-Verlag: Berlin, 1991.